

Optical wireless localization

Mehmet Bilgi · Abdullah Sevincer ·
Murat Yuksel · Nezih Pala

Published online: 5 November 2011
© Springer Science+Business Media, LLC 2011

Abstract In this paper, we explore the possibility of using directionality of free-space-optical (a.k.a. optical wireless) communications for solving the 3-D localization problem in ad-hoc networking environments. Range-based localization methods either require a higher node density (i.e., at least three other localized neighbors must exist) than required for assuring connectedness or a high-accuracy power-intensive ranging device such as a sonar or laser range finder which exceeds the form factor and power capabilities of a typical ad-hoc node. Our approach exploits the readily available directionality information provided by a physical layer using *optical wireless* and uses a limited number of GPS-enabled nodes, requiring a very low node density (2-connectedness, independent of the dimension of space) and no ranging technique. We investigate the extent

and accuracy of localization with respect to varying node designs (e.g., increased number of transceivers with better directionality) and density of GPS-enabled and ordinary nodes as well as messaging overhead per re-localization. Although denser deployments are desirable for higher accuracy, our method still works well with sparse networks with little message overhead and small number of anchor nodes (as little as 2). We also present a proof-of-concept prototype of our FSO-based localization techniques and show the validity of our approach even with three transceivers per node.

Keywords Free-space-optics · Ad-hoc networks · Spherical FSO structures · Localization

This work is supported in part by NSF awards 0721452 and 0721612 and by DARPA under contract W31P4Q-08-C-0080. Nezih Pala was with Omega Advanced Solutions, Inc. during the earlier part of the work presented in this paper. An earlier version [1] of this work appeared in IEEE GLOBECOM Workshop on Optical Wireless Communications, 2011.

M. Bilgi · A. Sevincer (✉) · M. Yuksel
CSE Department, University of Nevada, MS 171, 1664 N.
Virginia Street, Reno, NV 89557, USA
e-mail: asev@cse.unr.edu; asevincer@gmail.com;
abdullahsevincer@yahoo.com

M. Bilgi
e-mail: mbilgi@cse.unr.edu

M. Yuksel
e-mail: yuksem@cse.unr.edu

N. Pala
ECE Department, Florida International University, 10555 W
Flagler Street. EC 3910, Miami, FL 33174, USA
e-mail: npala@fiu.edu

1 Introduction

Providing contextual location information for the application-level data is a vital enhancement for ad-hoc networks. Localization capabilities are also important for network-level functionalities such as routing. Geographical routing protocols such as GPSR [2] are known to reduce the forwarding table sizes substantially, however, they need to know the location of nodes to do a successful ID-to-location mapping. Despite the strong need for localization, the task of localizing an ad-hoc node given its power capabilities, mobility, and other network parameters (e.g., node density, anchor density) is not trivial. Traditional approach of sensing the signal strength from 3 neighbors and triangulating using the derived distances requires a high neighbor density (3 localized neighbors) and is not accurate due to the multi-path loss in RF propagation. The issue becomes even more severe if the problem is considered in 3-D space, since then, it takes 4 nodes (reaching up to 2

times the normal node density) to triangulate and even more samples (preferably from different neighbors) for calibration and better accuracy [3]. Sonar and laser range finder devices are not suitable for the power capabilities and form factors of ad-hoc nodes and explicit bearing devices are space consuming. Alternatively, we propose to use the *directionality that is inherent in FSO communication* which does not impose any additional hardware requirements. In our approach, a node can calculate its location given that it has 2 neighbors that know their own location, and advertise their location and interface normals in the packets that they transmit. Our method is lightweight in comparison to range-based methods since it *only requires 2 localized neighbors* and it *does not involve a complex tuning phase*.

We considered FSO as a complementary communication mechanism to aid in increasing the overall network throughput in [4]. Previous studies revealed that FSO-only mobile ad hoc networks are viable and using *auto-alignment* circuitry and protocol, line-of-sight issues can be remedied significantly [5–8]. However, FSO communication technologies has not been used to solve the ad-hoc localization problem and they provide a substantial amount of potential as it is quite efficient to run triangulation algorithms using *direction of reception* (i.e., angle of arrival). We use directionality of FSO beams to identify the angle of arrival (Fig. 1). By using *advertised normals* in packet headers, we can then calculate the relative angular orientation of neighbors with respect to each other. Since a node can receive packets (with advertised normal information in them) from more than 2 neighbors, we need to choose which information sets to use while triangulating.

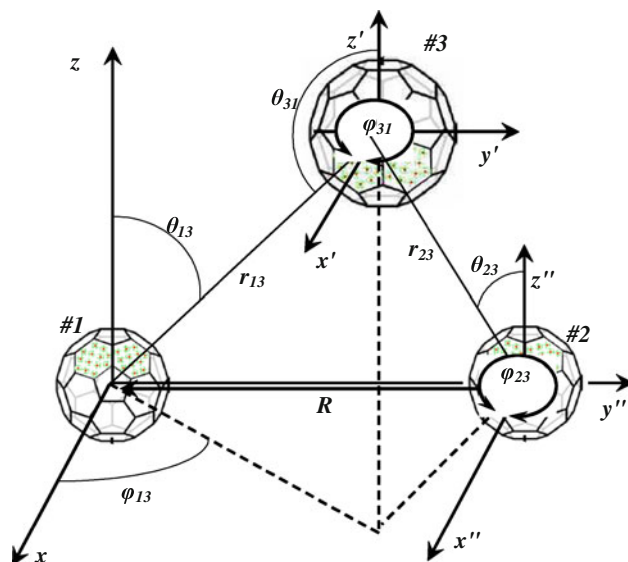


Fig. 1 A third node triangulating using the advertised normals received from two other localized or GPS-enabled nodes

We suggest and compare three different heuristics to make this selection.

Key characteristics of our FSO-based solution are:

- Capability of localization in 3-D,
- Much less power consumption in comparison to techniques requiring RF hardware,
- Only two localized neighbors are needed, which reduces the node density requirements, and
- Fast heuristics to select a subset of neighbors to use for localization.

Besides these three different heuristics, we also provide a proof-of-concept prototype implementation for a basic FSO-based localization scenario. In this scenario, we used three nodes (two stationary and one mobile) each with three FSO transceivers, and showed that a mobile third node can localize itself by exchanging FSO-based messages with the other two stationary nodes even though it is moved to 7 different locations on an arc of a semi circle with varying diameter values.

The rest of the paper is organized as follows: we present a background for the related work in localization in ad-hoc networks in Sect. 2. Section 3 presents our implementation of a basic triangulation algorithm in NS-2 network simulator [9]. In Sect. 4, we discuss the heuristics in detail. We present the simulation results for different scenario setups in Sect. 5. In Sect. 6 we present the details of our prototype implementation with the 7 different experiment locations and results and finally summarize our work.

2 Background: Ad-Hoc localization

Problem of node localization has been tackled by various methods: using ranging techniques [10–12], bearing techniques [13], and combination of the two [3, 14]. Robotics and image community has been working on the localization problem using landmark detection techniques and laser range finders [15–17]. However those methodologies are less practical for ad-hoc network localization due to either power requirements or lack of a camera in an ad-hoc node.

Range-based methods require at least 3 localized nodes (4 in a 3-D setting) to enable localization of a fourth node with varying degrees of quality. Major limitation of range-only methods is that they require high density of nodes to achieve high localization coverage. SpotON [10] and Calamari [11] systems build on the assumption of a simple path propagation model with known parameters for RF whereas this does not hold in practical environments where multi-path propagation is the norm especially in indoor settings to score a 10% error in ranging even after an intense calibration process.

Niculescu considers angle-of-arrival as the approach for triangulation without the need for any ranging measurements [13]. Their approach requires additional hardware for detecting the angular placement of neighbor nodes (such as an antenna array or a sonar device). They conclude that angle-of-arrival (AOA) methods can have accuracy that is comparable to range-based methods. However, requirement for additional RF hardware results in large structures with potentially high power consumption and is impractical for many ad-hoc networking settings.

Akella proposed a hybrid technique [18] that uses optical wireless (FSO) combined with ranging techniques. They require only one localized neighbor relaxing the node density requirement considerably. The method is appropriate especially for low-density and intermittently connected networks with accuracy trade-offs. However, their need for range measurement is, although achievable using signal strength measurements, requires extra computational complexity and it is prone to measurement errors.

A key characteristic of our solution is to use *optical-only techniques* to achieve localization. Our method requires much less power availability than RF-based methods, and is particularly useful for ad hoc networking settings where line-of-sight exists among low-power nodes. Our proposition provides high localization extent with as little as only 2 localized or GPS-enabled nodes with acceptable accuracy through the use of narrow transceivers when 2-connectness requirement is satisfied.

3 System model

The 2 types of nodes are: anchor nodes with GPS devices and ordinary nodes that do not know their locations initially. Network nodes with a GPS device send control packets including their location and direction information so that the immediate neighbors without a GPS device can use the transferred information to find their own locations. These control packets convey the *advertised normals*, which include sender node's ID, if sender has a GPS device, if sender has previously triangulated, hop distance of sender from the nearest anchor node (localization rank), if the sender node has previously triangulated, and transmit antenna's global location and its direction (normal). The receiver of such a packet stores this information in a table (mapping from node ID to localization information) with the arrival time of the packet as presented in Algorithm 1.

One can derive simple algebraic equations:

$$r_{31} = \frac{R}{\sin \theta_{31} (\tan \varphi_{31} + \tan \varphi_{32})} \sqrt{1 + \tan^2 \varphi_{31}} \quad (1)$$

$$r_{32} = \frac{R}{\sin \theta_{32} (\tan \varphi_{31} + \tan \varphi_{32})} \sqrt{1 + \tan^2 \varphi_{32}} \quad (2)$$

$$\begin{aligned} X_3 &= X_1 + r_{13} \sin \theta_{13} \cos \varphi_{13} \\ Y_3 &= Y_1 + r_{13} \sin \theta_{13} \sin \varphi_{13} \\ Z_3 &= Z_1 + r_{13} \cos \theta_{13} \end{aligned} \quad (3)$$

that give the location of a third node. The distance between two GPS-enabled nodes is R (Nodes 1 and 2). From this distance and θ and φ angles that are derived from the transmitter normal advertisements in packet headers, we can calculate r_{31} and r_{32} (Equations 1 and 2). Lastly, we need to conduct simple vector additions to find the coordinates of Node 1.

Localization rank of a node is the hop distance of that node from the nearest anchor node. As depicted in Fig. 2(a), node C has rank 0 indicated as a subscript. When a node without a GPS device triangulates, it's rank is the maximum of the ranks of sender nodes added by 1. Hence if a node is next to 2 GPS-enabled nodes (each with rank 0) and it triangulates using the information that it received from these two nodes, it will have rank 1. Such a ranking mechanism helps us prioritize the available information while triangulating. Intuitively, if we consider a network with uniform geographical distribution of nodes and anchor nodes placed at the center, nodes that are in the skirt of the network will have the highest ranks. Moreover, nodes with higher ranks are subject to larger localization errors.

A node is "ill-connected" when the number of directly reachable neighbors is less than 2. Hence, we require a node to be in transmission proximity of at least 2 direct neighbors even though it may not be able to transmit and receive from those neighbors because of line-of-sight issues. Thus, upon starting to place ordinary nodes (without GPS devices), we place the anchor nodes at arbitrary locations. For example, if number of GPS-enabled nodes in X axis is 2 and in Y axis is 3, we divide the X edge of the determined area into 3 and Y edge into 4 equal lengths and place one anchor node at the end of each X - Y edge with another corresponding anchor node placed on the same point with a given Z value. Hence a pair of GPS-enabled nodes are placed on top of each other with some distance in Z axis. We acknowledge that such a requirement on the placement of anchor nodes can limit the applicability of our approach. However, one can come up with placement methodologies that relax such strict placement requirements and ensure that a subset of surrounding non-anchor nodes have 2 connections to separate GPS-enabled nodes.

While placing non-anchor nodes, we consider a candidate location drawn from 3 uniform randoms for X , Y , and Z coordinates. We check if there are at least 2 nodes within the communication range of the candidate location. If so, we accept the candidate location and move to the next node. If we assume that there is only one pair of GPS-enabled nodes in the network, rest of the nodes form a

Algorithm 1 Relative Localization

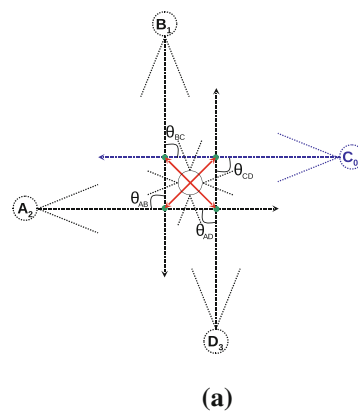
```

1:  UPON Reception Of Packets With Localization Header:
2:  if This Node Has At Least 2 Neighbors' Advertised Normals
    AND
    It Is Not A GPS-Enabled Node then
3:      Determine Which 2 Localization Information Sets To
        Use
        Via One Of The Heuristics
4:      if Using Most Recent Sets To Triangulate then
5:          FIND 2 Latest Received Localization Packets
6:      end if
7:      if Using Angular Priority then
8:          FIND 2 Localization Packets That Make An Angle
        Closest To 90°
9:      end if
10:     if Using Localization Rank then
11:         FIND 2 Localization Packets With Minimum Ranks
12:     end if
13:     CALCULATE Closest-Point-Of-Approach Of The 2
        Rays
14:     UPDATE This Node's Location
15:     UPDATE This Node's Localization Rank
16:     UPDATE This Node's State Flag As "Triangulated"
17:     START Stamping Outgoing Packets
18: end if

```

sphere-like cluster in 3-D space. Moreover, when we increase the number of GPS-enabled node pairs to 2, we introduce the possibility of creating two disconnected clusters and enable the nodes to be placed in a larger volume, which in turn may decrease localization extent in the network because of line-of-sight issues involved. The only strict requirement while placing anchor nodes is that they are *placed as pairs*, on top of each other, which ensures that a third node that is able to see both nodes can localize itself.

Fig. 2 Amplification of localization error in time and error in different heuristic models. **a** A simplified triangulation in 2D using two GPS-enabled nodes and error in default LOS model. **b** Localization errors are being amplified during the simulation when two latest received information sets are used for triangulation

**4 Heuristics**

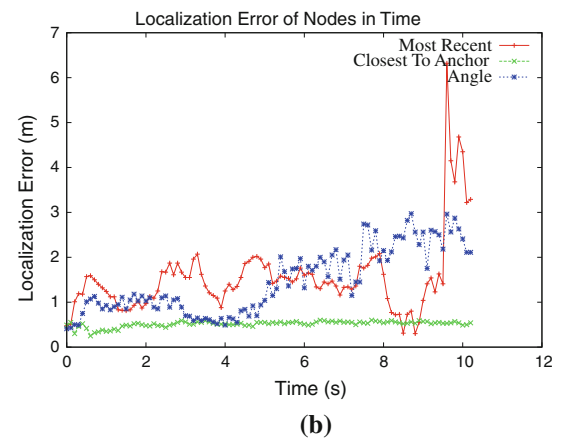
In our study, we found that it is possible to employ a number of *simple heuristics* while deciding which two information sets to use for triangulation from a given number of information sets. Possible number of different ways to localize is $\binom{n}{2}$ where n is the number of information sets available to a given node.

4.1 Stale info gets forgotten

Possibly the simplest heuristic is to use the information that became available the latest. Assuming a node can use 4 different localization information sets as depicted in Fig. 2(a), the triangulating node will select the latest two arrivals. Observe that localization error is amplified throughout the network with this heuristic. Since each node re-triangulates as it receives a packet using the most up-to-date information, node will consider the latest information no matter how far the sender node is to the closest anchor. Hence, even though more accurate information is available, the choice results in increased localization errors as can be seen in Fig. 2(b). We found that the best triangulation result is obtained at the first attempt since the received localization information sets have been propagating from anchor nodes towards the nodes with higher ranks at skirts of the network.

4.2 Lower the rank the better

In this heuristic, we first assign a “localization rank” of 0 to a GPS-enabled node. When a node triangulates using localization information obtained from two neighbors, it attains the localization rank of maximum of the two neighbors added by 1. If we assume that the network has only one pair of GPS-enabled nodes and the distribution of



the nodes form a sphere-like shape in 3-D, nodes that are closer to the core where the two anchor nodes reside, will have lower localization ranks and the outer skirts of the network will have larger localization ranks indicating that they are more distant from the core in number of hops. Hence, when a node is about to decide the pair of neighbors for triangulation, it may choose them in such a way that summation of the two ranks is minimized. This heuristic ensures that neighbors that are closest to anchor nodes are selected for triangulation. Figure 2(a) shows nodes' ranks as subscripts. Assuming the node in the middle is triangulating, it will select the information sets that came from C_0 and B_1 since they have the lowest ranks.

4.3 Angular prioritization

One of the hard cases to triangulate using only directionality information is when the triangulating node lies on the straight line that passes through the both two nodes (collinearity). Results become more accurate when the two nodes are chosen in such a way that they attain a certain angle between each other (e.g., 90°). Throughout our experiments we found that one major factor that was causing increased localization error was ill-formed (flat) triangles that were the result of unwisely chosen 2 candidate information sets. A natural way to remedy the problem is to impose a lower bound on the angle between the two nodes (e.g., $0.005 * \pi$) and favor those sets making an angle close to 90° (orthogonality, in 3-D). Figure 2(a) shows θ_{BC} , θ_{AB} , θ_{AD} and θ_{AD} angles made by all 4 nodes. Assuming θ_{BC} is closest to 90° , the triangulating node will choose information sets sent by node B and node C for triangulation.

5 Performance evaluation

We looked at a number of metrics while justifying the performance of our approach. The first metric is initial localization error. Initial localization error indicates the *aggregate absolute difference* between calculated location and actual location of all nodes in the network. This metric is calculated for a node when it localizes itself for the first time. Nodes in the network continue to re-localize themselves as they receive more packets. We stop the simulation when all the nodes are localized or simulation time reaches 10 s, whichever happens first. Since the simulated network is stationary, 10 s is enough as an upper bound for simulation duration. We calculate final localization error using the last calculated locations of each triangulated node before the simulation ends because of either of the reasons. Another metric that needs to be considered is final localization error averaged by the number of all localized nodes.

5.1 Comparison of heuristics

We ran simulations of 100 nodes with 14 interfaces on each for 10 iterations using each heuristic. Each interface had a divergence angle of 600 mrad ($\sim 34^\circ$). There were 8 GPS-enabled nodes (making 4 pairs) and all nodes were placed on the 3-D volume randomly. We found that selecting the latest information set gives the worst results since the error is neither predictable nor close to a desired level. Similarly, angular prioritization gives elevated localization errors as well but still better than selecting the latest information sets and is relatively stable. Among the 3 heuristics, the one based on localization ranking resulted the lowest localization error per-node as depicted in Fig. 2(b). Hence, throughout the rest of the simulation sets, we used this ranking based heuristic to determine which 2 sets to use for triangulation.

5.2 Node density

Our second simulation set is designed to determine the effect of node density in the network on localization extent. For this experiment we increased the number of nodes from 32 to 288. There are 26 interfaces with 400 mrad of divergence angle on each node. There are 16 anchor nodes in the network and all of the ordinary nodes are placed randomly on a 3-D terrain. We ran the simulation setup for 5 iterations and averaged the results. As depicted in Fig. 4(b), we found that as we increase the node density, the localization extent first gets higher, but later reduces as more neighbors start falling into their blind regions (i.e., no line-of-sight) and start becoming obstacles to each other. A similar trend is observed in localization error (Fig. 4(a)) as well. However, the final per-node localization error steadily benefits from more neighbors.

5.3 Anchor density

In Fig. 3(a), (b), one can see that in a simulation of 100 nodes, when the number of GPS-enabled nodes is increased from 4 to 40, both *aggregate* and *per-node* localization errors decrease. Also, it is an important observation that the localization extent makes a significant jump from 2 pairs (4 nodes) to 4 pairs. However, increases after that point reduce the localization extent. We conclude that because of the scattering effect of the random node placement algorithm, the volume that the nodes are distributed is increased, which in turn makes the LOS a more significant problem.

5.4 Divergence angle

Figure 4(c) shows the how divergence angle affects the overall and per-node localization error. As we increase the

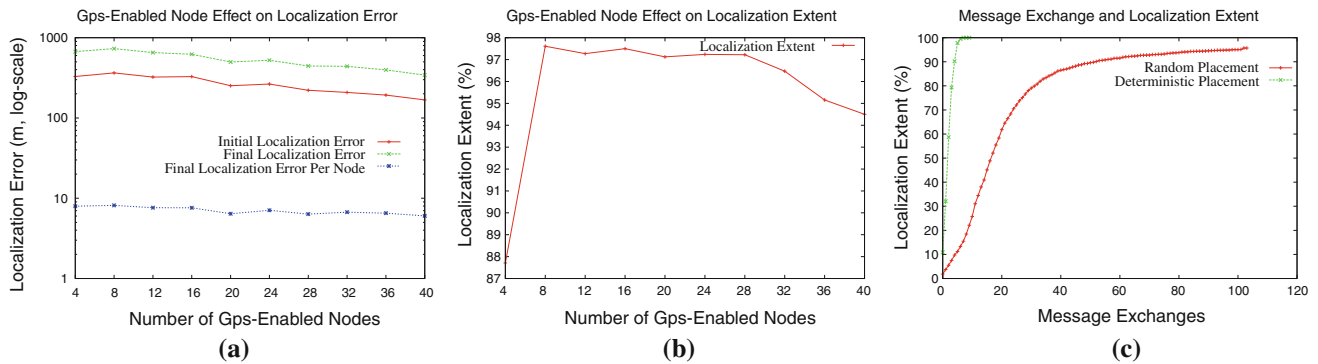


Fig. 3 Effect of number of GPS-enabled node on localization error and localization extent and message exchange overhead

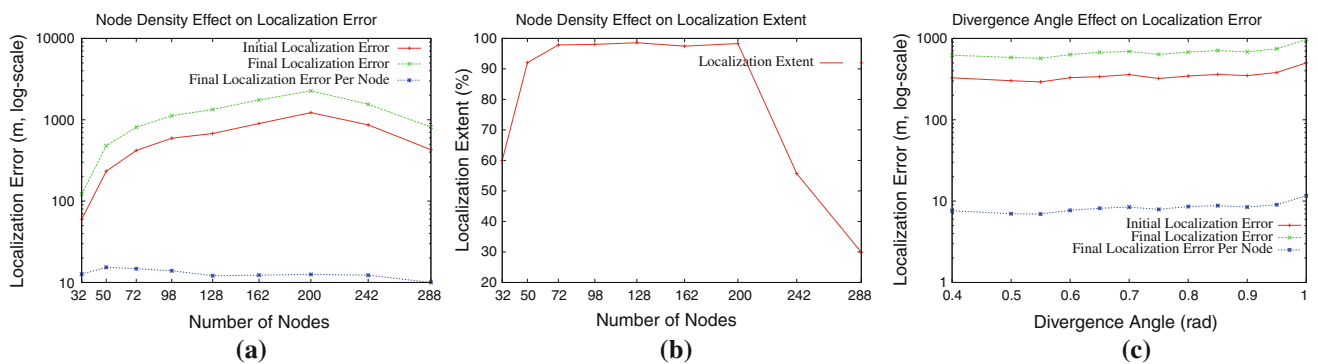


Fig. 4 Effect of node density on localization error and localization extent and different node designs with varying divergence angles

divergence angle, it reduces the accuracy of the default-normal estimates. Hence, the localization error is increased. We conclude that designing multi-element optical antennas with more transceivers on them not only increases throughput [4], but it also increases the accuracy of localization.

5.5 Message overhead and localization extent

A key practical metric is how long it takes the whole network to localize. In this set of simulations, we investigated the localization extent after each message exchange. We used 200 nodes each with 26 transceivers using 400 mrad divergence angle. There were 8 GPS-enabled nodes and we ran the simulations for 10 iterations. We ran two separate simulation setups for this scenario. In the first setup, we placed the nodes on a $10 \times 10 \times 2$ perfect grid and in the second setup, we placed all the nodes randomly. As depicted in Fig. 3(c), we saw that placement of nodes on the terrain is a significant factor in extent of localization and message exchange overhead. First setup with deterministic placement reaches over 90% localization extent in 10 message exchanges. However, the setup with randomly placed nodes reaches 90% after 90 message exchanges and 80% after 33 message exchanges.

6 Prototype experiments for basic localization scenario

In this section we present a proof-of-concept prototype of our FSO-based localization technique. The prototype consists of two main parts, namely transceiver circuit and controller circuit. We used commercially available off-the-shelf optoelectronic components in the market to build the prototype.

6.1 Transceiver circuit

The transceiver circuits contains one infrared LED, one photo-detector (PD), and a simple biasing circuit on a circular-shaped board. The diameter of each transceiver board is 25 mm. A picture of the transceivers are shown in Fig. 5. As shown in Fig. 6, each transceiver is connected to a controller board that implements the localization algorithm. We used different types of infrared LEDs from different manufacturers in order to make measurements and alignment more reliable. Most of the LEDs that we use are GaAlAs double heterojunction LEDs with varying peak emission wavelengths of 850–950 nm. We observed that most of the infrared LEDs' signals reflect from walls in an indoor environment which makes measurements



Fig. 5 Optical antenna with transceivers and SFH 4881 is replaced on to transceivers

unreliable and difficult. We tried to find LEDs with very narrow divergence angle in order to make more sensitive measurements of angle-of-arrival. We measured each LED's divergence angle by using our transceiver circuit, since the conditions in which the measurements are done to gather these LEDs' specifications by manufacturers may be different than our lab conditions. So, we measured the divergence angle of each LED with our transceiver circuit also considering reflections in our indoor environment. Among 12 different LEDs we selected SFH 4881 [19], which is reliable and has a fabricated liquid phase epitaxy process. The angle of half intensity is stated ± 5 in the data sheet and in our experiments we measured the angle of half intensity of SFH 4881 at about ± 16 . This was the most reliable and stable LED in our lab experiments. SFH4881 consumes low power. The maximum ratings for the forward current is 200 mA according to its specifications [19]. The power consumption of the LED is approximately 15 mW when it is driven with a forward current of 100 mA. We measured the forward current as 13 mA and the forward voltage as 1.2 V for our prototype. The power consumption of one LED is approximately 1.56 mW. It is possible to use different LEDs with less power consumption to optimize the prototype for a power critical scenario. In this paper, since our focus is prototyping the localization algorithm, we have not optimized the prototype design for power consumption. It is an interesting future work direction to explore the trade-offs in designing multi-transceiver FSO structures with minimal power consumption.

The signal that is sent from the micro-controller is modulated by PIC12f615 [20] at 455 kHz carrier frequency and sent to the LEDs. At the receiving side, we used TSOP7000 series [21] for receiving modulated signals.

TSOP7000 is a miniaturized receiver for infrared remote controller devices and IR data transmission. A PIN diode and preamplifier are assembled on a lead frame and the epoxy package is designed as an IR filter. The received signal can directly be decoded by the micro-controller. With these features, the receiver side of the transceiver circuit is capable of receiving localization frames that is sent from other nodes in its neighborhood.

6.2 Controller circuit

The controller board contains a micro-controller which is responsible for alignment detection and sending localization information to the aligned transceivers. Each controller board is connected to 3 transceivers pointing towards different directions. The controller board also includes the micro-controller and a transistor which is responsible for driving emitting diode at desired modulation frequency. A line transceiver which is responsible to convert TTL logic levels to RS232 is added to the controller board in order to establish communication with a laptop computer's serial port. We used the PIC24FJ128GA106 [20] for implementing an alignment algorithm [8] that automatically detects availability of line-of-sight alignment with neighbor nodes. The controller circuit shown in Fig. 6 is responsible for searching for possible alignments, simultaneous data transmission and sending localization packets through multiple transceivers.

6.3 Alignment and localization algorithm

FSO communication is prone to mobility and it requires establishment and maintenance of line-of-sight (LOS) between FSO transmitters since FSO transceivers are highly directional. Therefore, we first implemented a simple LOS detection and establishment protocol which uses a three-way handshaking routine in order to detect transceivers that are in line-of-sight of each other. [8] By this protocol we are able to send localization packets to the appropriate transceiver.

The essence of our LOS alignment protocol is to exchange small frames between neighboring FSO nodes and identify the transceivers that are in each other's line-of-sight. The protocol aims to establish a *bi-directional* optical wireless link and hence uses a simple three-way handshake messaging method for full assurance of the alignment. Our alignment protocol uses a small frame of 4 bytes. Hence a frame does not keep the physical channel busy for too long. A frame starts with a FRAME_START byte, indicating the start of channel usage by another transceiver. SENDER_ID and RECEIVER_ID fields follow the frame indicator. Both bytes are node IDs instead of transceiver IDs. Last byte is the FRAME_TYPE byte that

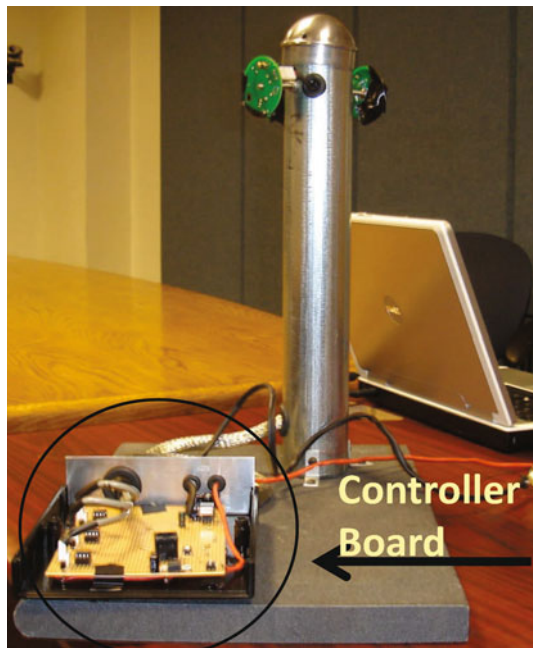


Fig. 6 Picture of controller board

indicates the intention of the sender of this frame. The re-alignment algorithm starts by sending SYN frames through a particular transceiver. Lets assume A.1 on node A. The algorithm keeps sending this initial signal periodically until it receives a SYN_ACK answer to its SYN or it receives a SYN originated from a transceiver on a different node than itself: B.1 on node B. If it receives a SYN, it replies with a SYN_ACK. If it receives a SYN_ACK, it replies with an ACK. For simplicity, let us follow the case in which that A.1 sends a SYN, B.1 replies with SYN_ACK and A.1 replies with an ACK. When A.1 sends out its first ACK frame it changes internal state to ALIGNED with node B and same is true for B when it receives the ACK. At this point, B and A starts exchanging DATA frames. We did not implement an ACK mechanism for DATA frames to keep the protocol simple. In a frame of type DATA, the fifth byte is the length of the payload. Hence, the payload length is variable. On a localization packet the payload length is 6. First three bytes are the coordinates of the X, Y, Z location of the node that is sending the localization packet. The second three bytes are the normal values of the corresponding transceiver that is sending the localization packet. If a node receives two different localization packets from different nodes, it calculates the location information using Closest-Point-Of-Approach Of The 2 Rays approach [22]. After 2 s the alignment timer goes off and changes the state of the interface to SENDING_SYN which starts the alignment process again. This simple alignment process, although exchanges a very small number of frames, will disrupt the carried flow and cause drops. The algorithm

has been successful in establishing the alignment at the first trial, that is with exchange of only 3 frames.

6.4 Experiments

We implemented a simple FSO transceiver and alignment circuit prototype which exchanges localization packets among corresponding transceivers that are in line-of-sight of each other. The micro-controller connects to a laptop computer (A) through RS-232 serial port. This micro-controller implements the alignment algorithm: it routinely probes for new alignments. Localization packets can only be sent to one node by another node when the alignment is established between corresponding transceivers. This simple prototype is replicated for 2 other laptop computers labeled B and C, so that we can send localization packets among three nodes/laptops.

We implemented a software running on the laptop PCs which we can configure the node locations and normals (the relative angle that a transceiver is pointing to) of the transceivers that a node corresponds. When the alignment is established, localization packets are sent at this initial configuration setup. We have to pre-configure the normals when we turn a node since the relative angle that the transceiver is pointing to changes.

Our goal in experimental setup is to show that it is possible to achieve localization by using directionality of the free-space-optical communication in ad-hoc environments. In this setup, we use three nodes with three transceivers, and show that it is possible to achieve localization even with three transceivers per node. We envision packaging of tens of transceivers per node and achieving practical and highly accurate localization. Two of the three nodes in our setup stays at a fixed position when the third node is moving on an arc of a semi-circle. We have established two experimental setups: 2 and 3 m experiments. In the first setup, i.e., the 2 m *experiment*, we placed Node-A and Node-B 4 meters apart which is the the diameter length of the semi-circle on which Node-C travels. The center of the diameter is the center of the coordinate system, i.e., the location (0,0). Considering this coordinate system, Node-A is placed at location (2,0) and Node-B is placed at location (−2,0), as shown in Figs. 7 and 10. Node-C was moved among 7 different locations on the arc of this semi-circle. Starting at Node-B's location, each location on the arc has 22.5 degrees angle difference with respect to the coordinate (0,0). Fig. 8 shows the placements of the nodes in the experiment setup. We used SFH 4881 in our experiments which has 15 degrees angle of half intensity measured at our lab experiments. Thus, there were blind spots in the arc of this semi-circle which we didn't receive localization packets. We turned around

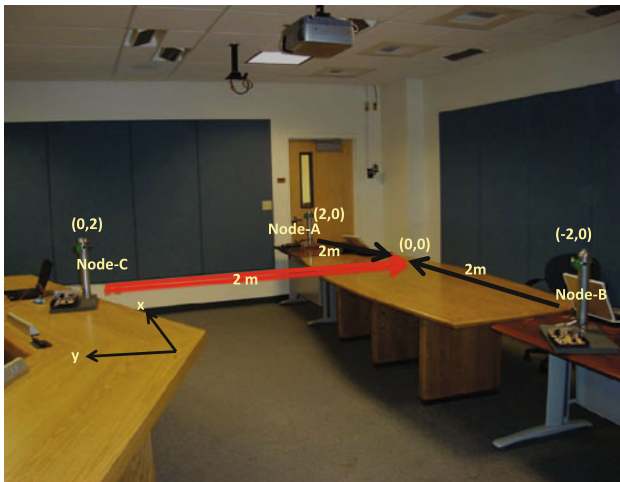


Fig. 7 2 m experiment setup: Node-C is perpendicular to the diameter

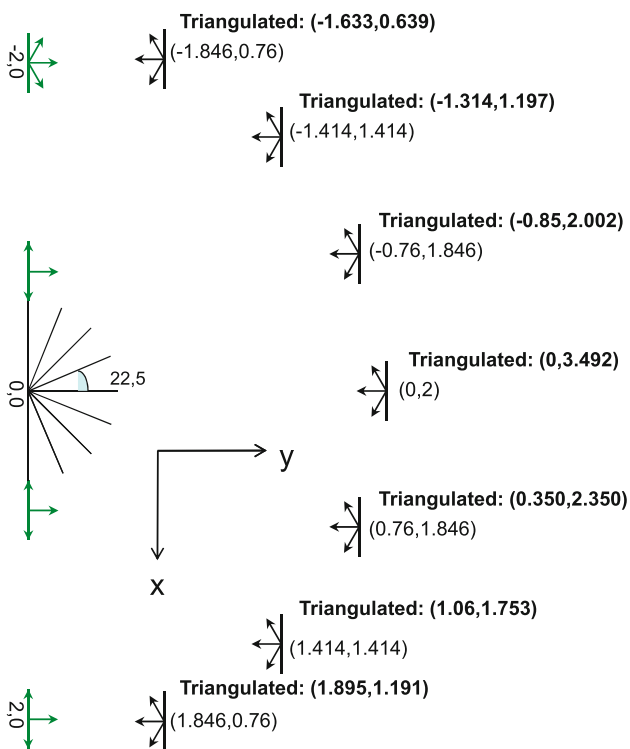


Fig. 8 Experiment setup: The actual locations and triangulated locations for the 2 m setup. Node-C is placed at 7 different locations

each node in order to establish the alignments so that localization packets were received by the three nodes for each of the 7 arc locations. We calculated normals of the aligned transceivers and calculated the location of Node-C by applying the Closest-Point-Of-Approach Of The 2 Rays approach described in Section 6.3. In our second experiment setup, i.e., the 3 m experiment, we increased the

diameter of the arc to 6 m. Similar to the first setup, we placed Node-A at location (3,0) and Node-B at location (-3,0). Node-C was moved among 7 different locations with a radius of 3 and 22.5 angle difference starting at point B, as shown in Fig. 9. The number of blind spots that we have in this setup is increased compared to the previous setup. We were also able to receive localization packets in this setup at the 7 different locations although finding the critical points when turning over the transceivers to get localization packets were not as easy as in the previous setup. Based on the experiments, we calculated three different error values. The first error value is based on the error at x axis which is the absolute value of the difference between the actual location of Node-C at x axis and the triangulated location at x axis (Equation 4). The second error value is based on the error at y axis. We again took the absolute value of the difference between the actual location at y axis and the triangulated location at y axis (Equation 5). Third error value is the distance between the actual (x, y) location of the node and the triangulated (x, y) location of the node (Equation 6). We can formalize our error values as follows:

$$\text{Error}_x = |X_{\text{actual}} - X_{\text{Triangulated}}| \quad (4)$$

$$\text{Error}_y = |Y_{\text{actual}} - Y_{\text{Triangulated}}| \quad (5)$$

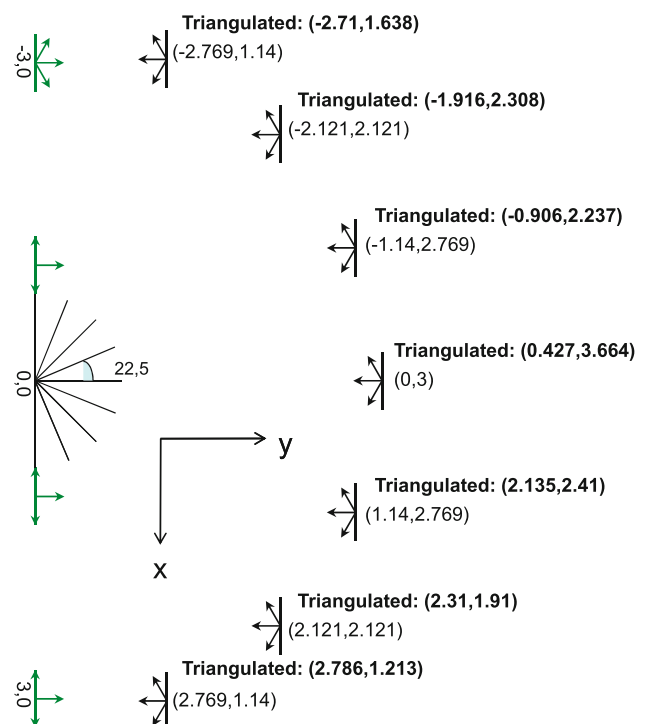


Fig. 9 Experiment setup: The actual locations and triangulated locations for 3 m setup. Node-C is placed at 7 different locations

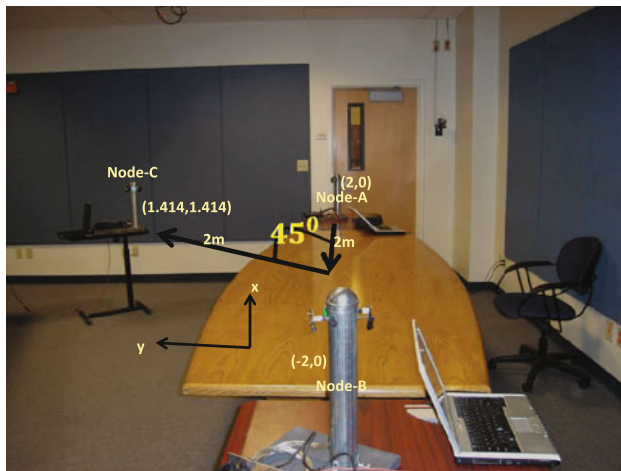


Fig. 10 2 m experiment setup: Node-C is placed at 45 degree with x axis

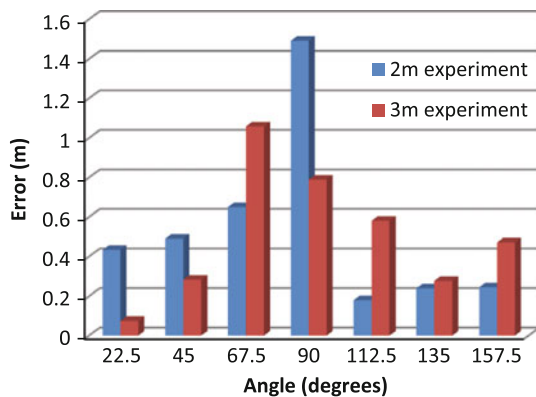


Fig. 11 Error behavior between two points for the 2 and 3 m experiments at corresponding angle values

$$\text{Error}_{xy} = \sqrt{(X_{\text{actual}} - X_T)^2 + (Y_{\text{actual}} - Y_T)^2} \quad (6)$$

Figures 11 and 12 show the error values at corresponding angle values for 2 and 3 m experiment setups. As can be seen from the Fig. 11, there is an increase at error rates when Node-C is placed on the y axis, meaning that the angle between the x axis and the node is 90 degrees, i.e., they are perpendicular. Error rates decrease when the node is moved to the left or right of this point. Figure 12 shows that the error during the 2 m experiment was less than the error during the 3 m experiment at some points, and vice versa. Larger diameter seems to favor locations closer to the 90 degrees location, i.e., when Node-C is closer to the y axis. For both diameter values, there is an increase at error values when we are close to the y axis. Since the error values of the 2 and 3 m experiments are pretty close to each other, it is not possible to define a clear difference based on the diameter.

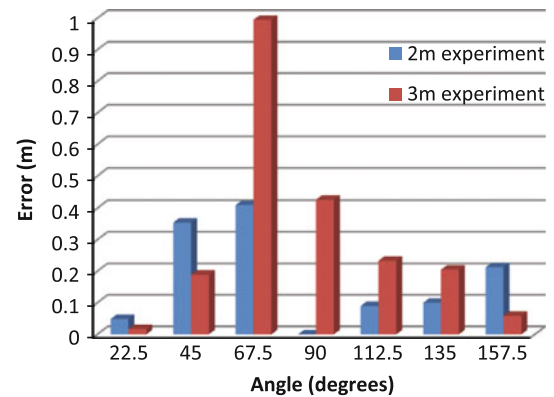


Fig. 12 Error behavior at x axis for the 2 and 3 m experiments at corresponding angle values

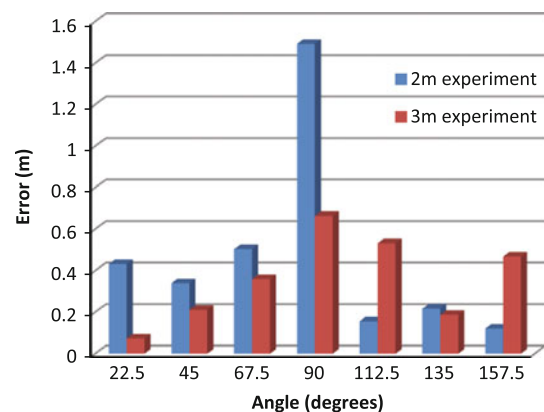


Fig. 13 Error behavior at y axis for the 2 and 3 m experiments at corresponding angle values

7 Summary

We proposed a novel approach to the problem of node localization in the context of ad-hoc networking via multi-element free-space-optical antennas. We used readily available directionality information to perform a simple triangulation. Our approach is lightweight in processing needs, does not need a complex tuning phase, and is stingy in terms of required extra hardware. We showed that optical wireless is attractive because of both its high throughput and easy-to-exploit directionality benefits that are helpful in solving the localization problem.

We implemented our optical wireless localization approach on a proof-of-concept lab prototype and illustrated that the localization error can be kept under control even with three transceivers per node. Since optoelectronic components can be densely packaged, we envision nodes with tens of transceivers. Such densely packaged multi-transceiver nodes can use transmitters and photo-detectors with very narrow divergence angles, and thus achieve very

accurate angle-of-arrival detection, which is not possible via using RF signals.

Future work includes adding more transceivers with very small divergence angles on the current working prototype and considering long range localization scenarios. Due to their high speed modulation capability, such multi-transceiver FSO communication systems are also attractive as an approach complementary RF communication in the next generation wireless networks. Compared to other localization techniques requiring dense node deployments, a wireless system capable of both high speed data communication and accurate angle-of-arrival measurement able to localize itself with very low node density presents a great opportunity for designing devices able to perform more with less resources. These FSO systems also consume less power than other localization techniques and thus have significant usage potential for power critical environments like sensor networks.

References

1. Bilgi, M., Yuksel, M., & Pala, N. (2010). 3-d optical wireless localization. In *Proceedings of IEEE GLOBECOM 2010 Workshop on optical wireless communications*, December 2010.
2. Karp, B. (2000). GPSR: Greedy perimeter stateless routing for wireless networks. In *Proceedings of ACM/IEEE MobiCom 2000*, August 2000.
3. Chintalapudi, K. (2004). Ad hoc localization using ranging and sectoring. In *Proceedings of IEEE INFOCOM*, Hong Kong, China, March 2004.
4. Bilgi, M., & Yuksel, M. (2008). Multi-element free-space-optical spherical structures with intermittent connectivity patterns. In *Proceedings of IEEE INFOCOM Student Workshop*.
5. Yuksel, M., Akella, J., Kalyanaraman, S., & Dutta, P. (2009). Free-space-optical mobile ad hoc networks: Auto-configurable building blocks. *ACM Springer Wireless Networks*, 15(3), 295–312.
6. Bilgi, M., & Yuksel, M. (2010). “Packet-based simulation for optical wireless communication. In *Proceedings of IEEE Workshop on local and metropolitan area networks*. IEEE.
7. Bilgi, M., & Yuksel, M. (2010). Throughput characteristics of free-space-optical mobile ad hoc networks. In *Proceedings of ACM International conference on modeling, analysis and simulation of wireless and mobile systems*. Bodrum, Turkey: Sheridian Publishing, October 2010.
8. Sevincer, A., Bilgi, M., Yuksel, M., & Pala, N. (2009). Prototyping multi-transceiver free-space-optical communication structures. In *Proceedings of IEEE international conference on communications*, May 2009.
9. The Network Simulator NS-2. <http://isi.edu/nsnam/ns/>.
10. Hightower J., Vakili C., Borriello G., & Want R. Design and Calibration of the SpotON Ad-Hoc Location Sensing System.
11. Whitehouse, K., & Culler, D. (2002). Calibration as parameter estimation in sensor networks. In *WSNA '02: Proceedings of the 1st ACM international workshop on wireless sensor networks and applications*, pp. 59–67. New York, NY, USA: ACM, 2002.
12. Girod, L., & Estrin, D. (2001). Robust range estimation using acoustic and multimodal sensing. In *Proceedings of the 2001 IEEE/RSJ International Conference on Intelligent Robots and Systems*, 2001 (Vol. 3, pp.1312–1320). doi:10.1109/IROS.2001.977164.
13. Niculescu, D. (2003) Ad hoc positioning system (aps) using aoa. In *INFOCOM 2003*, pp. 1734–1743. Atlanta, GA, March 2003.
14. Akella, J., Yuksel, M., & Kalyanaraman, S. (2006). A relative ad hoc localization scheme using optical wireless. In *2nd International Conference on Communication Systems Software and Middleware, 2007 (COMSWARE 2007)* (pp. 1–8). doi:10.1109/COMSWA.2007.382580.
15. Bahl, P. (2000). RADAR: an in-building RF-based user location and tracking system. In *Proceedings of conference on computer communications (INFOCOM)*.
16. Raab, F., Blood, E., Steiner, T., & Jones, H. (1979). Magnetic position and orientation tracking system. *IEEE Transactions on aerospace and electronic systems* AES-15(5), 709–718, September. 1979.
17. Krumm, J., Harris, S., Meyers, B., Brumitt, B., Hale, M., & Shafer, S. (2000). “Multi-camera multi-person tracking for easyliving”. *IEEE Workshop on Visual Surveillance*.
18. Akella, J., Yuksel, M., & Kalyanaraman, S. (2007). “A relative ad-hoc localization scheme using optical wireless,” in *Proceedings of IEEE/Create-Net/ICST international conference on communication system software and middleware (COMSWARE)*.
19. Osram opto semiconductors. (2010). <http://www.osram-os.com/>.
20. Microchip technology inc. (2010). <http://www.microchip.com/>.
21. Vishay-manufacturer of discrete semiconductors and passive components. (2009). <http://www.vishay.com/>.
22. Distance between lines and segments with their closest point of approach. http://www.softsurfer.com/Archive/algorithm_0106/algorithm_0106.ht.

Author Biographies



Mehmet Bilgi has received his Ph.D. from the CSE Department of The University of Nevada, Reno (UNR) in December 2010. During his studies at UNR, he has worked on simulation of multi-element free-space-optical MANETs under the supervision of Dr. Murat Yuksel. His research focused on throughput capacity of FSO-MANETs, relative localization using orientation-only methodologies, and prototyping such systems. His research interests are in the

computer networks and distributed systems area in general. He received his M.S. degree from UNR in May, 2008 and B.S. degree from Computer Engineering Department of Fatih University, Istanbul, Turkey in June, 2005. He is a member of IEEE.



Abdullah Sevincer is a Ph.D. student at the CSE Department of The University of Nevada, Reno (UNR) and he is working under supervision of Dr. Yuksel. His current research focuses on several aspects of multi-element free-space-optical mobile ad-hoc networks including throughput analysis and comparison, prototyping and localization. His research interests are in computer networks area. He received his M.S. degree from UNR in 2010 and B.S. degree from

Electrical Engineering Department of Yildiz University, Istanbul, Turkey in 2004. He is a member of IEEE and ACM.



Murat Yuksel is currently an Assistant Professor at the CSE Department of The University of Nevada - Reno (UNR), Reno, NV. He was with the ECSE Department of Rensselaer Polytechnic Institute (RPI), Troy, NY as a Postdoctoral Research Associate and a member of Adjunct Faculty until 2006. He received a B.S. degree from Computer Engineering Department of Ege University, Izmir, Turkey in 1996. He received M.S. and Ph.D. degrees from

Computer Science Department of RPI in 1999 and 2002 respectively. His research interests are in the area of computer communication networks with a focus on protocol design, network economics, wireless routing, free-space-optical mobile ad-hoc networks (FSO-MANETs), and peer-to-peer. He is a member of IEEE, ACM, Sigma Xi, and ASEE.



Nezih Pala received his B.S. degree from Middle East Technical University, Ankara, Turkey in 1996 with honors, M.S. and Ph.D. degrees in Electrical Engineering from Rensselaer Polytechnic Institute, Troy, NY in 1999 and 2002, respectively. Prior to joining The Electrical and Computer Engineering Department of FIU, he has been working as senior research scientist at Sensor Electronic Technology, Inc. and Visiting Scholar at Rensselaer Polytech-

nic Institute. His research interests include design, fabrication and characterization of nanoscale energy harvesting and storage systems, electronic and optoelectronic devices, plasmonics THz devices and applications particularly in biological and chemical sensing. Dr. Pala authored/coauthored 30 articles published in peer reviewed scientific journals and 34 papers presented in conferences. His paper on δ THz Plasmonic Detectors for Biodetection received Paper of the Month Award in December 2008 from the journal of Electronics Letters. He is also recipient of Best Paper Award of MRS Fall 1999 meeting. Dr. Pala is a member of IEEE, The International Society for Optical Engineering (SPIE), Material Research Society (MRS), Eta Kappa Nu, Tau Beta Pi and Sigma Xi. He also serves in the organizing committee of SPIE Conferences.